

Quantum plasmons in the hybrid nanostructures of double vacancy defected graphene and metallic nanoarrays

Rui Tang(唐睿), Yang Xu(徐阳), Hong Zhang(张红), and Xin-Lu Cheng(程新路)

Citation: Chin. Phys. B, 2021, 30 (**1**): 017804. DOI: 10.1088/1674-1056/abaedb
Journal homepage: http://cpb.iphy.ac.cn; http://iopscience.iop.org/cpb

What follows is a list of articles you may be interested in

High performance terahertz anisotropic absorption in graphene-black phosphorus heterostructure

Jinming Liang(梁晋铭), Jiangtao Lei(雷江涛), Yun Wang(汪云), Yan Ding(丁燕), Yun Shen(沈云), Xiaohua Deng(邓晓华)

Chin. Phys. B, 2020, 29 (**8**): 087805. DOI: 10.1088/1674-1056/ab9cbf

Broadband strong optical dichroism in topological Dirac semimetals with Fermi velocity anisotropy

J Lim(林镇杰), K J A Ooi(黄健安), C Zhang(涨潮), L K Ang(洪礼祺), Yee Sin Ang(洪逸欣)

Chin. Phys. B, 2020, 29 (**7**): 077802. DOI: 10.1088/1674-1056/ab928e

Acoustic plasmonics of Au grating/Bi_2Se_3 thin film/sapphirehybrid structures

Weiwu Li(李伟武), Konstantin Riegel, Chuanpu Liu(刘传普), Alexey Taskin, Yoichi Ando, Zhimin Liao(廖志敏), Martin Dressel, Yuan Yan(严缘)

Chin. Phys. B, 2020, 29 (**6**): 067801. DOI: 10.1088/1674-1056/ab8a3c

Processes underlying the laser photochromic effect in colloidal plasmonic nanoparticle aggregates

A E Ershov, V S Gerasimov, I L Isaev, A P Gavrilyuk, S V Karpov

Chin. Phys. B, 2020, 29 (**3**): 037802. DOI: 10.1088/1674-1056/ab6551

Large-scale control of enhancement and quenching of photoluminescence for ZnSe/ZnS quantum dots and Ag nanoparticles in aqueous solution

Shaoyi Yin(殷少轶), Liming Liao(廖李明), Song Luo(罗松), Zhe Zhang(张喆), Xiaoyu Zhang(张晓宇), Jian Lu(鹿建), Zhanghai Chen(陈张海)

Chin. Phys. B, 2019, 28 (**5**): 057803. DOI: 10.1088/1674-1056/28/5/057803

Quantum plasmons in the hybrid nanostructures of double vacancy defected graphene and metallic nanoarrays*

Rui Tang(唐睿)[1], Yang Xu(徐阳)[2], Hong Zhang(张红)[1,3,†], and Xin-Lu Cheng(程新路)[2,3]

[1] College of Physics, Sichuan University, Chengdu 610065, China

[2] Institute of Atomic and Molecular Physics, Sichuan University, Chengdu 610065, China

[3] Key Laboratory of High Energy Density Physics and Technology of Ministry of Education, Sichuan University, Chengdu 610065, China

(Received 10 July 2020; revised manuscript received 3 August 2020; accepted manuscript online 13 August 2020)

We study the plasmonic properties of hybrid nanostructures consisting of double vacancy defected graphene (DVDGr) and metallic nanoarrays using the time-dependent density functional theory. It is found that DVDGr with pure and mixed noble/transition-metal nanoarrays can produce a stronger light absorption due to the coherent resonance of plasmons than graphene nanostructures. Comparing with the mixed Au/Pd nanoarrays, pure Au nanoarrays have stronger plasmonic enhancement. Furthermore, harmonics from the hybrid nanostructures exposed to the combination of lasers ranged from ultraviolet to infrared and a controlling pulse are investigated theoretically. The harmonic plateau can be broadened significantly and the energy of harmonic spectra is dramatically extended by the controlling pulse. Thus, it is possible to tune the width and intensity of harmonic spectrum to achieve broadband absorption of radiation. The methodology described here not only improves the understanding of the surface plasmon effect used in a DVDGr-metal optoelectronic device but also may be applicable to different optical technologies.

Keywords: plasmon, double vacancy defected graphene, mixed metallic nanoarrays, multi-beam laser, harmonic spectrum

PACS: 78.20.Bh

DOI: 10.1088/1674-1056/abaedb

1. Introduction

Surface plasmons (SPs), excitations in metal nanostructure, can break the diffraction limit of nanometer level.[1,2] This excellent property can be used in many aspects such as optical nano-antenna,[3] catalytic reactions,[4] optical waveguides,[5] molecular electronics,[6] and optical biosensors.[7] However, the SPs in metal is liable to decay during propagation, and the SPs in metal devices is relatively simple and can not be effectively modulated. Graphene is one-atom-thick two-dimensional layers of sp^2-bonded carbon, which has many advantages, e.g., exceptionally high crystal and electronic quality,[8] ultrahigh carrier mobility,[9] and wide range of light absorption,[10] and can be controlled by the grating.[11,12] In particular, compared with metal nanostructure, the plasmon on the surface of the graphene has some more excellent properties. The most one is a relatively long propagation distance with a light decay.[13,14] Therefore, graphene can make up the drawbacks of noble metals in SPs, for example, it can replace noble metals for optical signal transmission.[15,16] Recently, the research result of Abajo *et al.* indicated that when the graphene scale is down to the molecular size, the layout of the resonance frequency of plasmon can be extended to visible light and ultraviolet range.[17] The photoelectric devices made of graphene have been experimentally obtained, such as photoelectric detectors, ultrafast laser, and optical modulator.[18–20]

At present, graphene has been experimentally prepared by a number of methods.[21–23] Due to the limitation of manufacturing process, all sorts of defects inevitably appear in graphene, including Stone–Wales defects, vacancy defects, absorption defects, etc.[24–26] One of the most typical and common defects is double vacancy defects (DVDs) (as shown in Fig. 1).[27,28] The defects would change graphene's properties just like the enhancement of the activity of graphene substrate,[29] prone to the stable adsorption of different molecules or atoms on its surface,[30] breaking the symmetry of graphene,[31] inducing magnetism,[32] and also destroying the metal properties and enhancing the semiconductor properties. Numerous methods have been used for observing the grain boundaries and defects in graphene sheets, for example, transmission electron microscopy,[33,34] atomic force microscopy, scanning tunneling spectroscopy[35] and scanning tunneling microscopy.[36] Although there are several methods to detect the defects, they have some shortcomings such as the need for complex sample preparation, taking up more time, and a limited observation range. Furthermore, much less attention is paid to DVDGr than defect-free graphene, and there is no research on plasmons of DVDGr neither theoretical nor experimental, while the DVDGr is so common in applications. Therefore, theoretical research for DVDGr plasmons

*Project supported by the National Key R&D Program of China (Grant No. 2017YFA0303600) and the National Natural Science Foundation of China (Grant Nos. 11974253 and 11774248).

†Corresponding author. E-mail: hongzhang@scu.edu.cn

© 2021 Chinese Physical Society and IOP Publishing Ltd

has important guiding significance for practical applications of graphene.

Theoretical calculations have predicted the presence of collective plasmon modes in a few atom chains of several metallic elements: Na,[37] Ag,[38] and Au;[39] see, for example, Ref. [40] for a review. In a previous study,[41] plasmon–exciton interactions in a monolayer graphene–Ag nanoparticle hybrid system were systemically investigated. The experimental results demonstrated that the surface catalytic reactions can not only be controlled by plasmon–exciton coupling, but also be affected by the gate voltages and electric currents (or bias voltages). With a fabricated electro-optical device based on a hybrid of graphene–Ag nanoparticles, Lin *et al.* studied plasmon–exciton codriven oxidation reactions. It is found that the most contribution to the oxidation reaction is from hot holes on graphene, controlled by the gate voltage and the bias voltage.[42] Nayyar *et al.* examined the role of transition-metal (TM) doping in the generation of plasmon modes in a single Au chain. It was found that doping leads to several additional excitations in the absorption spectrum reflecting changes in the potential around the TM atom and collective effects of the "localized" (TM d-) and delocalized (s) electrons.[43]

The linear and nonlinear optical absorption properties of TwBLG have been carefully studied. This generalized analysis method of electric field and magnetic field separation shows that Moire pattern can precisely regulate the distribution of TMDM to control the chirality of TwBLG.[44] However, the linear and nonlinear optical absorption properties of the double vacancy defected graphene and metallic nanoarrays have not been fully studied theoretically. In this paper, we present first-principles calculations of quantum plasmons in the DVDGr–gold hybrid nanostructures. When we put the DVDGr flake and gold wire together, the interaction between the light and graphene will become stronger. This can produce stronger plasmons in the visible ranges.[45–47] We address some of the fundamental questions about the nature of collective excitations in nanostructure plasmons by considering an arrangement of mixed metallic nanoarrays. The optical properties of both pure and "mixed" arrays of free-standing homonuclear chains are calculated using the time-dependent density functional theory (TDDFT). We also study the harmonics from the hybrid nanostructures exposed to the combination of lasers ranged from ultraviolet to infrared and a controlling pulse. Our simulation results may provide beneficial information for plasmons in a practical DVDGr-gold nano-device and the detection of defects on graphene.

2. Computational details

All calculations were performed using the real-space and real-time TDDFT code OCTOPUS,[45] and the carbon, hydrogen and gold atoms were described by the Troullier–Martins pseudopotentials.[48] Local-density approximation (LDA)[49] for the exchange-correlation was used in both the ground state and excited state calculations as employed by Marinopoulos *et al.*[50] To obtain the linear optical absorption spectrum, the system was excited by a δ-function impulse in the initial state. Then the Kohn–Sham wave functions were propagated for some time. The simulation zone was defined by assigning a sphere around each atom with a radius of 6 Å and a uniform mesh grid of 0.3 Å. In the real-time propagation, the excitation spectrums were extracted by Fourier transform of the dipole strength, and the electronic wave packets were evolved for typically 6000 steps with a time step of $\Delta t = 0.003$ $\hbar$/eV.

Different types and shapes of time-dependent external perturbations are applied to the system, in the form of

$$f(x,y,z)\cos(\omega t+\phi(t))g(t),$$
$$g(t_1) = F_0\cos\left[\frac{\pi}{2}\frac{t_1-2\tau_0-t_0}{\tau_0}\right],$$
$$g(t_2) = G_0\exp[-(t_2-t_0)^2/2\tau_0^2],$$

where $f(x,y,z)$ is defined by a field type and polarization or a scalar potential, cosine controls the waveform, ω controls the frequency, and $\phi(t)$ is the time-dependent phase. The $g(t)$ function centered around t_0 describes the waveform of the ultrafast laser.

To calculate nonlinear optical properties, we follow the evolution of the system under the influence of a laser field that is treated in the dipole approximation. The harmonic emission spectrum can then be calculated from the acceleration of the dipole moment:

$$H(\omega) \propto \left|\int \mathrm{d}t\, \mathrm{e}^{\mathrm{i}\omega t}\frac{\mathrm{d}^2}{\mathrm{d}t^2}\mathrm{d}(t)\right|^2.$$

3. Results and discussion

3.1. Plasmons in the planar hybrid structures

Comparing the plasmon in defect-free graphene flake and DVDGr flake, we demonstrate that DVDs have an effect on the light absorption and change the charge distribution in graphene surface. Figures 1(a) and 1(d) indicate that the absorption peak at the high-energy modes shows a large blueshift and reduces markedly. For considering the optical application of DVDs, we just focus on the low-energy modes (less than 5 eV). As shown in Figs. 1(b) and 1(c), charge density distribution of graphene and DVDGr in the low-energy modes performs differently. The tunnel effect changes due to the surface charge distribution changes in the DVDGr for the lack of a few carbon atoms compared with the perfect graphene. When the impulse excitation is polarized along the zigzag edge, the charge is separated from the hole (Figs. 1(e) and 1(f)). The direction of the incident light exerts a crucial influence on the graphene plasmon due to the long-range charge transfer excitation of SPs in low energy region. Along the direction of

excitation, electrons can vibrate back and forth over a long distance. Thus, we can detect whether or not there are defects in graphene by comparing the spectrum and the induced charge density with defect-free graphene.

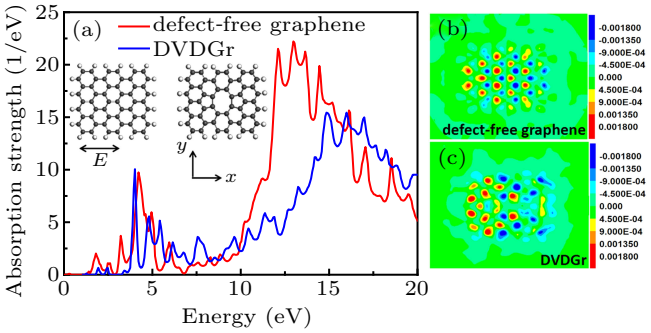


Fig. 1. (a) Optical absorption of DVDGr flake and defect-free graphene flake. The impulse excitation is polarized along the armchair edge (parallel to the x-axis); (b) and (c) Fourier transform of the induced charge density for defect-free graphene and DVDGr, at the energy resonance points 4.19 and 4.02 eV, respectively. (d) Optical absorption of DVDGr flake and defect-free graphene flake. The impulse excitation is polarized along the zigzag edge (parallel to the y-axis). (e) and (f) Fourier transform of the induced charge density for defect-free graphene and DVDGr, at the energy resonance points 4.08 and 4.83 eV, respectively.

To acquire a more particular knowledge of the electron behavior, we study the plasmon in a series of hybrid systems by placing a DVDGr sheet and the Au wires together named as DVDGr-AuX, where X ($X = 2$, 3, 4, and 5) represents the number of Au atoms on each side of DVDGr. As shown in Fig. 2, the edges of DVDGr are passivated with hydrogen atoms, and the distance between the nearest gold atom and the hydrogen atom was set to 2.89 Å according to the experimental results of Nilius *et al.*[51]

Figures 2(b)–2(d) show the optical absorptions of four DVDGr-AuX ($X = 2$, 3, 4, and 5) with resonance absorptions at 3.51, 2.95, 2.33, and 2.06 eV, respectively. The close absorption frequencies of isolated DVDGr (black curve) and isolated Au nanoarrays (red curve) lead to enhancement light absorption of DVDGr-AuX (blue curve) by resonance. The results illustrate vividly that the collective nature of the excitations is ascertained by the strong absorption peak. The free electrons can be transferred between the rectangular DVDGr flake and the Au cluster, and the local electromagnetic field will also be enhanced. Moreover, the gold antennas convert the incident light into plasmon accompanied by the enhancement of the electromagnetic field, and this strong near-field can directly excite the hole-electron pair in the defective graphene. As more Au atoms are added, the position of resonance absorption peak is red-shifted about 1.5 eV and the value is raising about 17 eV^{-1} in total. The reason for selected enhancement is the coherent superposition of DVDGr-AuX' SPs and the increase of carrier concentration. These processes lead to an increase in carrier concentration, and further affect the optical response. More importantly, the enhancement modes can be chosen by the resonant frequencies of gold wires. The coherent superposition effect will enhance the absorption peak obviously. In order to confirm the above viewpoint, Figs. 2(e)–2(h) display the Fourier transform of the induced charge density for the four hybrid structures at the energy resonance points. In a previous work, Niu *et al.* suggested that an antiparallel dipole will be formed in the graphene because of the electromagnetic field coupling between graphene and Au nanoparticles.[52] We apply this explanation to our hybrid structures of DVDGr and gold wires. When the resonance frequencies are very close to each other, this electromagnetic coupling will evolve into plasmon coherence resonance. In addition, it can be seen that the induced charge in the DVDGr is mainly localized at the boundaries, and different modes correspond to similar spatial charge distributions. The edge state in graphene layer plays a vital role in optical response and plasmon modes.[53]

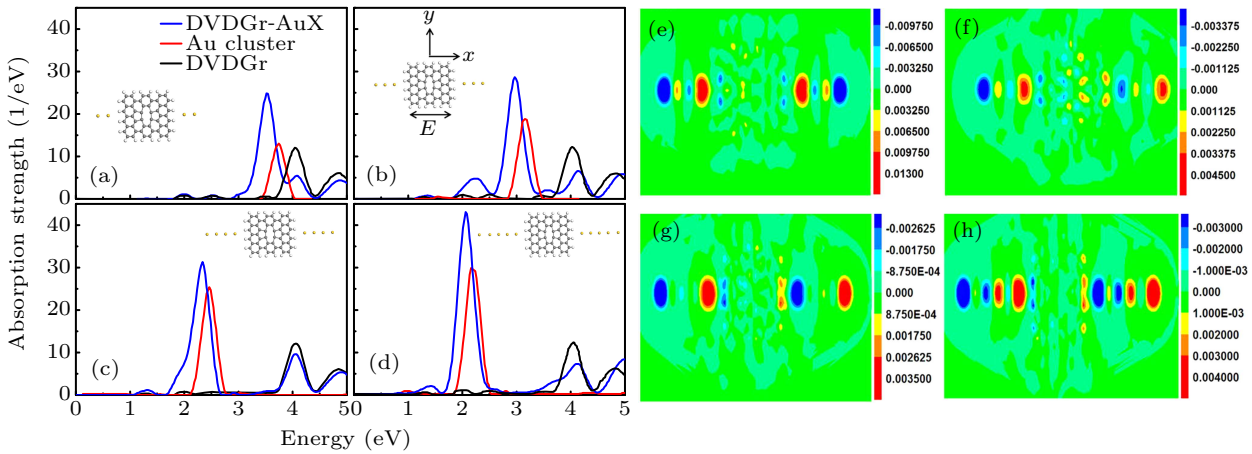


Fig. 2. Optical absorption of DVDGr-AuX consisting of the same DVDGr flake and different Au atoms: (a) DVDGr-Au2, (b) DVDGr-Au3, (c) DVDGr-Au4, and (d) DVDGr-Au5. The impulse excitation is polarized along the armchair edge. For comparison, the absorptions of the isolated DVDGr flake and the isolated gold wires are represented by a black curve and a red curve, respectively. Fourier transform of the induced charge density for the DVDGr-AuX: (e) DVDGr-Au2, (f) DVDGr-Au3, (g) DVDGr-Au4, and (h) DVDGr-Au5, at the energy resonance points 3.51, 2.95, 2.33, and 2.06 eV, respectively.

3.2. Plasmons of the mixed noble metal-TM arrays with the double vacancy defected graphene in planar hybrid structures

The above-mentioned studies addressed that increasing the number of Au atoms further intensifies the optical absorption and causes a slowly saturating redshift. In contrast, considering an arrangement of mixed metallic nanoarrays, we put the DVDGr flake and Au cluster doped with TM atom Pd together, named as DVDGr-AuXPdY, where X ($X = 6$, 4, 4, and 2) and Y ($Y = 4$, 4, 2, and 2) represent the numbers of Au and Pd. The distance of 2.884 Å is employed between Pd and Au. The assignments of configuration and optical absorption of planar hybrid structures with impulse excitation polarizing along the armchair edge are shown in Fig. 3. Resonance absorption of four DVDGr-AuXPdY ($X + Y = 4$, 6, 8 and 10) is 4.40, 3.31, 2.64 and 2.37 eV, respectively. It is well understood that an interplay between spill out and interband polarization control the actual sign of the plasmon shift. Presumably, this redshift is related to electron spill out. The plasmon energy increases with the nanowire amount. However, in the situation of the planar arrays of 4 Au and 4 Pd clusters, the plasmon energy does not increase but moderately decreases. The non-monotonic behavior for the configuration, which differs from the pure Au cluster, is owing to the quantum mechanical confinement of the average electron density between the mixed noble metal cluster and transition metal cluster impacted by the introduction of Pd. The photoabsorption spectrum of the DVDGr-AuXPdY is significantly suppressed and fragmented compared to the DVDGr-AuX. Despite collective effects enhance, this weak damping slows the increase of the plasmon intensity, indicating that Au cluster doped with TM atom Pd can reduce the plasmon energy on account of the more effective screening by the TM Pd.

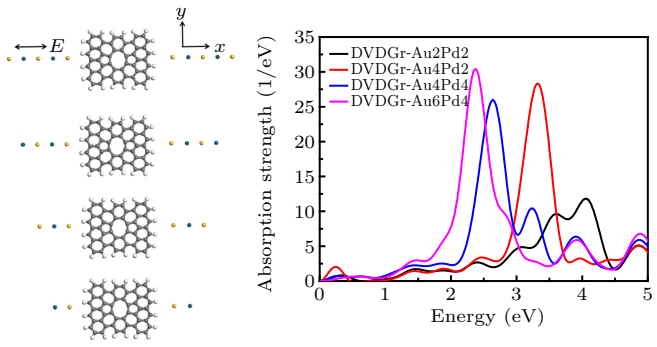


Fig. 3. Optical absorption of DVDGr-AuXPdY consisting of the same DVDGr flake and different Au, Pd clusters. The impulse excitation is polarized along the armchair edge. From bottom to top on the left: DVDGr-Au2Pd2, DVDGr-Au4Pd2, DVDGr-Au4Pd4, and DVDGr-Au6Pd10, respectively.

Leaving the impulse excitation polarized along zigzag edge, the plasmon blueshifts slightly with the increased number of clusters, as seen in Fig. 4. Resonance absorptions of four DVDGr-AuXPdY ($X + Y = 4$, 6, 8 and 10) at lower energy mode are located at 4.37, 4.34, 4.39 and 4.4 eV, respectively, and at higher energy mode they are 5.85, 6.36, 6.2 and 6.44 eV. Obviously, the doping of transition-metal generates additional excitations in the absorption spectrum, leading to the occurrence of double strong absorption spectrum. The optical absorption is broadened overwhelmingly that enables graphene-made quantum devices to have a wider range of light absorption spectra.

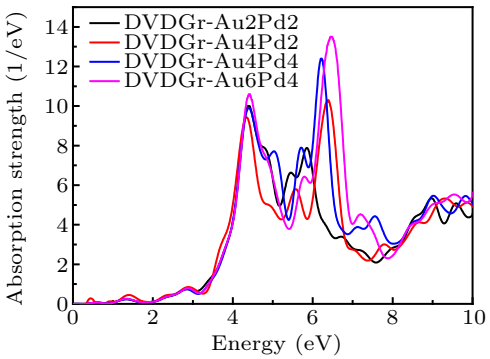


Fig. 4. Optical absorption of DVDGr-AuXPdY consisting of the same DVDGr flake and different Au, Pd clusters. The impulse excitation is polarized along zigzag edge. From bottom to top on the left: DVDGr-Au2Pd2, DVDGr-Au4Pd2, DVDGr-Au4Pd4, and DVDGr-Au6Pd10, respectively.

Compared with the mixed Au/Pd nanoarrays, pure Au nanoarrays have stronger plasmonic enhancement. Thus, the gold nanoarrays are expected to take as optical antenna, it presents a strong ability to capture visible lights.

3.3. Plasmons in non-planar hybrid structures

We analyze the evolution process of plasmon in the non-planar asymmetrical DVDGr-AuX which consists of a higher symmetry DVDGr (approximate hexagonal) and the different number of Au atoms–X ($X = 2$, 3, 4, and 5). The higher-symmetric DVDGr has a single shape boundary.[35] The gold wire is perpendicular to the DVDGr plane (yz plane) and it is mapped at the center of the octagon. The polarization direction of the incident light is maintained along the x-axis. Figure 5 displays the the DVDGr-Au5 hybrid structure and absorption spectrum of DVDGr-AuX ($X = 2$, 3, 4, and 5). The coupling excitation of photon and phonon (graphene plasmon) can result in photon-electron phonon interactions, which can significantly enhance resonance Raman scattering of mid-IR region, which is the so-called graphene plasmon-enhanced resonance Raman scattering of mid-IR region.[54] Focus on the optical absorption in mid-IR (below 1 eV) non-planar asymmetrical DVDGr-AuX structures, see Fig. 5. It is found that there is a new absorption peak in the infrared frequency ranges, which not only means that this non-planar hybrid structure has a very wide optical absorption but also makes clear that a new plasmon mode has appeared.

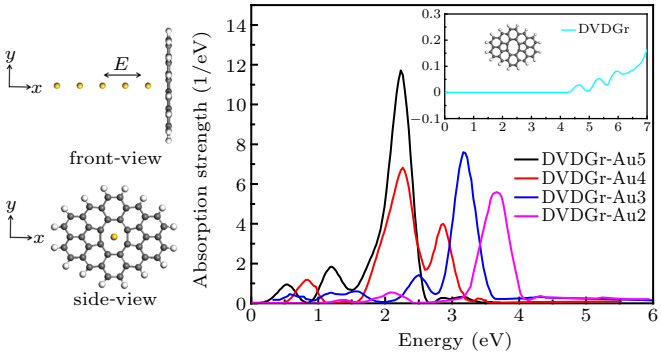


Fig. 5. Optical absorption of DVDGr-AuX consisting of the same DVDGr and the different numbers of gold atoms X ($X = 2$, 3, 4, and 5). The isolated DVDGr is displayed in the inset graphs.

We also analyze the plasmon of symmetrical DVDGr-AuX ($X = 2$, 3, 4, and 5). The polarization direction of incident light is along the x-axis. Figures 6(a)–6(d) display the optical absorption of the four symmetrical hybrid structures. Compared to the asymmetric structure, symmetrical hybrid structures present a pronounced peak in infrared frequency ranges, the peak value is rising a little. We can also find that the optical absorption spectra are wide in regard of visible, infrared or terahertz regions from Fig. 6(a)–6(d). Such wide ranges bring the non-planar symmetrical DVDGr-AuX a possibility to be used as an euryphotic photosensitive detector. Furthermore, increasing the number of Au atoms further intensifies the optical absorption and causes a new absorption peak in mid-IR (below 1 eV). The photoinduced charge transfer of DVDGr and Au can occur in electronic state transition of mid-IR region, and then the transferred electrons can interact with the phonon of DVDGr at mid-IR.

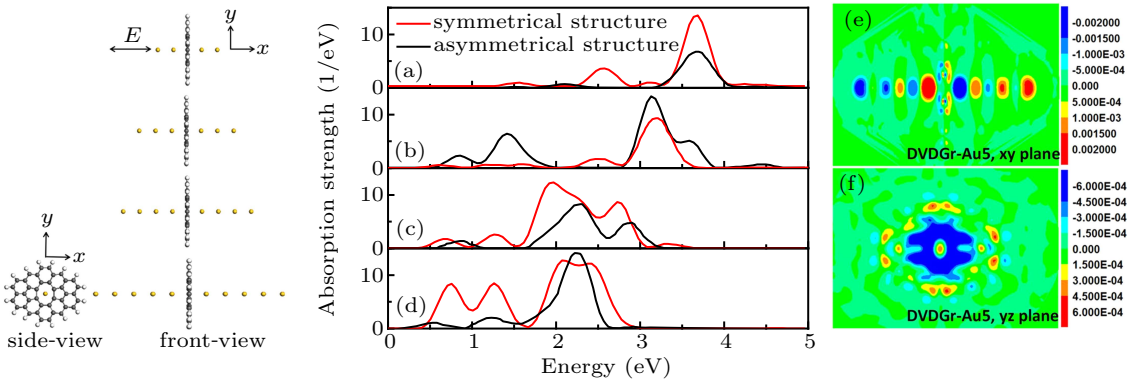


Fig. 6. Optical absorptions for non-planar symmetrical DVDGr-AuX ($X = 2$, 3, 4, and 5) shown in (a), (b), (c), (d). Red represents the higher symmetry DVDGr with different Au wires ($X = 2$, 3, 4, and 5), and black represents the asymmetrical DVDGr-AuX ($X = 2$, 3, 4, and 5). Fourier transform of the induced charge density for the DVDGr-Au5, at the energy resonance points 2.0 eV: (e) the xy plane, (f) the yz plane.

Figures 6(e)–6(f) show the Fourier transform of the induced charge density distribution of the symmetric DVDGr-Au5 in xy plane and yz plane. The polarization direction of incident light is perpendicular to DVDGr. The electrons are apparently clustered on the surface of graphene. Due to the shielding effect of interface charge, the antiparallel dipole appears on both sides of graphene, the electric field becomes weaker, and the peak value decreases.

Previous studies indicated that graphene boundary has a large effect on the plasmon mode and the light response and acts as a charge transfer channel. However, it is difficult to achieve such a function in the non-planar hybrid structure because it is very far away from the gold wire. Finally, the change of antenna size causes the variety of eigen frequency, which further results in a change of the optical response of the hybrid structure. Thus we can change the gold antenna to precisely regulate the range and intensity of the plasmon.

3.4. Plasmon-induced nonlinear responses

The couple's excitation between photon and phonon can result in the graphene plasmon, and the photon-electron-phonon interaction can result in the graphene plasmon-enhanced resonance Raman scattering, which can be enhanced up to 107 times.[54] Thus, we study the DVDGr plasmon-induced nonlinear responses to realize the extension and enhancement of the absorption. In this section, we adopt three kinds of incident laser beams to study the interaction of ultrafast lasers with DVDGr-Au5. The first and second for a Gaussian-like pulse and the third case for a totally diverse laser, as shown in Figs. 7(a), 7(c), and 7(e). Similar harmonic spectra are seen in Figs. 7(b) and 7(d) for the same choice of parameters but different amplitudes for the intensity. It is evident that the strength of the laser pulse constitutes important issues for the generation of harmonic. A dominant feature of the two spectra is the strong peak emitted at nearly the frequency that corresponds precisely to the plasmon frequency of DVDGr-Au5. For the case of the last one, the wavelength and intensity of the laser are chosen as $\lambda = 248$ nm and $I = 5.3 \times 10^{14}$ W/cm^2, respectively. An interesting feature of the spectra in Fig. 7(f) is that the harmonic gets excited at 15 eV due to nonlinear coupling with external perturbations.

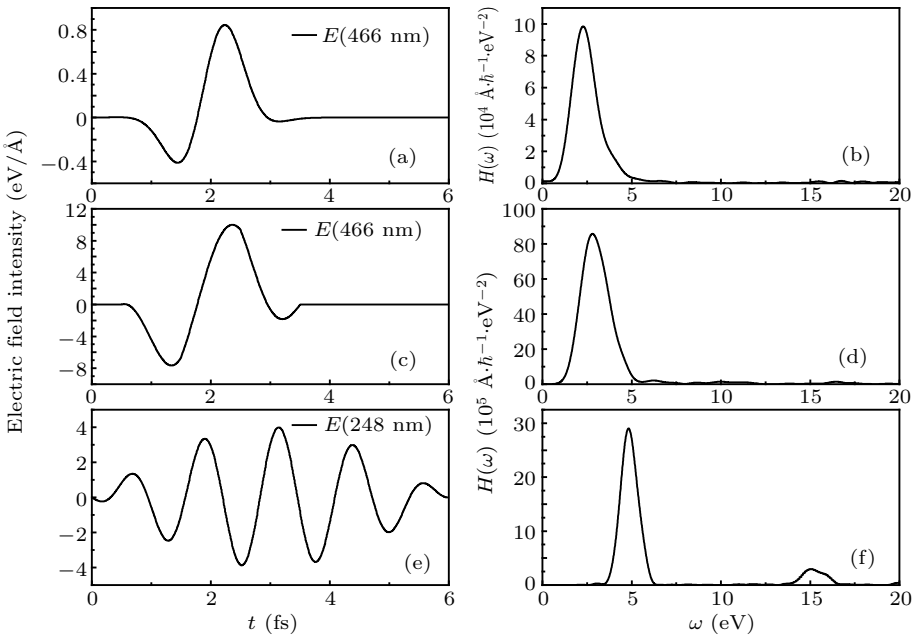


Fig. 7. Laser oscillograph and the corresponding harmonic spectra. Laser beams shown in (a), (c), (e) are for various wavelengths of 466, 466 and 248 (nm) and various intensities of 1.327×10^{14}, 1.327×10^{15}, 5.30×10^{14} W/cm^2.

To gain a deeper insight into DVDGr-Au5 plasmon-induced nonlinear responses, a set of simulations were performed with the purpose of exploring the effects of pulse shaping. The lasers ranging from ultraviolet to infrared with the same intensity corresponding to the center wavelengths of 138, 414 and 1379 nm respectively were chosen. Considering the momentously influence of the field intensity, four combined laser fields with peak intensity of 2×10^{13}, 6×10^{13}, 1×10^{14}, 1.45×10^{14} W/cm^2 were selected. Figure 8 shows the laser oscillograph with the intensity of 1.23 eV/Å. The actual effect of ultrafast laser is 6 fs.

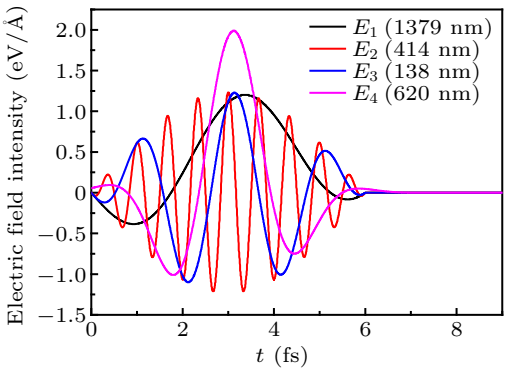


Fig. 8. Lasers with a controlling pulse oscillograph. Lasers with various wavelengths of 138, 414 and 1379 (nm) in the intensity of 1.23 eV/Å. Controlling pulse with the intensity of 2 eV/Å and wavelength of 620 nm.

The acceleration of the dipole moment is governed by the strength and the shape of the laser, hence the harmonic will be impacted dramatically by introducing a diverse type and shape laser as a modulation factor in a mixed field. As discussed above, Gaussian-like pulse can effectively boost the intensity of the harmonic spectrum. Thus, Gaussian-like pulses that performed as regulatory fields with the center wavelengths of 620 nm and peak intensity of 5.31×10^{13}, 8.97×10^{13}, 1.2×10^{14}, 1.63×10^{14} W/cm^2 are applied to the system. (Fig. 9 pink line).

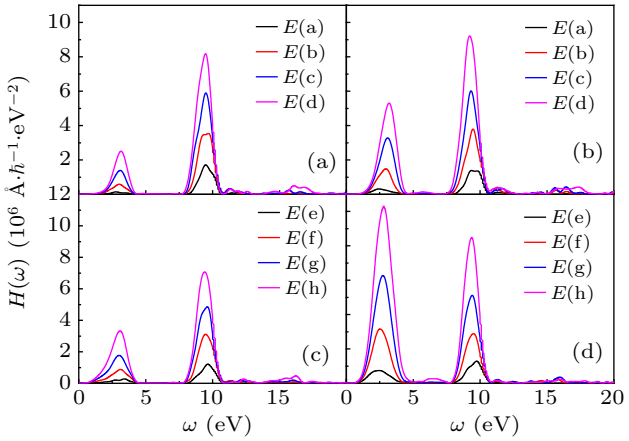


Fig. 9. Harmonic spectrum of DVDGr flake and DVDGr-Au5 obtained from the pulses in Figs. 8. (a) The DVDGr flake without Gaussian-like pulse. (b) The DVDGr flake with Gaussian-like pulse. (c) The DVDGr-Au5 flake without Gaussian-like pulse. (d) The DVDGr flake with Gaussian-like pulse.

In Fig. 9 we compare the harmonic spectrum of the DVDGr flake and DVDGr-Au5 obtained from the pulses in Figs. 8. The harmonic emission spectra show a double-plateau structure, the width increases mildly and the peak value boosts monotonously and non-negligibly with the augment of field intensity. We observe that, for the case in which the laser pulse is shaped, the harmonic at high energy mode can be excited, the electron energy varies according to the modulation of the laser electric field. Comparing the plasmon-induced nonlinear responses in DVDGr flake and DVDGr-Au, we note that the Au has the effect of enhancing harmonics in low-energy mode while suppressing emission in high-energy mode. A straightforward interpretation of these simulations is that the emission

can be tuned by the resonant frequency of gold nanoarrays. We also find that the emission is instructive in comparison with the harmonic generated from lasers with and without the laser electric field shaped by a Gaussian envelope. As shown in Fig. 9(d), the double-plateau of the harmonic spectrum is extraordinarily increased. In particular, the peak value in low energy mode even exceeds that in high energy mode. The latter introduces sharp spectral features characterized by the controlling laser, implying that changing the wavelength of the controlling laser can touch its quantum path, boost the specific harmonic peak. Furthermore, the modulation of the field brings about the spectrum becoming much smoother for the harmonics after the second plateau. This complexity provides an opportunity to tune nonlinear optical properties by combining disparate type and shape of external perturbations.

4. Conclusions

This work provides the first detailed theoretical analysis of DVD-Gr with multiple pure and mixed noble/TM nanoarrays using TDDFT. Effects of different structure on absorption spectrum and effects of various electronic field on harmonic spectrum have been investigated. It is noted that by adding metallic nanoarrays on double vacancy defected graphene plane, the plasmons produce coherent superposition, which enhances the absorption. This makes it possible to tune the plasmons in the hybrid nanostructures. The gold nanoarrays are expected to as optical antenna, and it presents a stronger ability to capture visible lights than mixed Au/Pd nanoarrays. Furthermore, DVDGr-Au plasmon-induced nonlinear responses suggest that for moderately intense femtosecond lasers, harmonic emission corresponds approximately to the plasmons frequency. We provide an effective method to realize the extension and enhancement of specific peak for the harmonic. This study is helpful to build a theoretical basis for understanding the microscopic mechanism of plasmon-induced nonlinear response and achieving ultimate control at the nanoscale.

Acknowledgment

We thank ShiJia Yuan and Tong Liu for fruitful discussions.

References

[1] Maiera S A and Atwater H A 2005 *J. Appl. Phys.* **98** 011101
[2] Karalis A, Lidorikis E, Ibanescu M, Joannopoulos J D and Soljacic M 2005 *Phys. Rev. Lett.* **95** 063901
[3] Novotny L and Hulst N 2011 *Nat. Photon.* **5** 83
[4] Bell A T 2003 *Science* **299** 1688
[5] Maier S A, Kik P G and Atwater H A 2002 *Appl. Phys. Lett.* **81** 1714
[6] Halas N J, Lal S, Chang W S, Link S and Nordlander P 2011 *Chem. Rev.* **111** 3913
[7] Cao Y W C, Jin R and Mirkin C A 2002 *Science* **297** 1536
[8] Geim A K and Novoselov K S 2007 *Nat. Mater.* **6** 183
[9] Chen J H, Jang C, Xiao S, Ishigami M and Fuhrer M S 2008 *Nat. Nanotechnol* **3** 206
[10] Ju L, Geng B, Horng J, Girit C, Martin M, Hao Z, Bechtel H A, Liang X, Zettl A, Shen Y R and Wang F 2011 *Nat. Nanotechnol.* **6** 630
[11] Mak K F, Sfeir M Y, Wu Y, Lui C H, Misewich J A and Heinz T F 2008 *Phys. Rev. Lett.* **101** 196405
[12] Nair R R, Blake P, Grigorenko A N, Novoselov K S, Booth T J, Stauber T, Peres N M R and Geim A K 2008 *Science* **320** 1308
[13] Jablan M, Buljan H and Soljacic M 2009 *Phys. Rev. B* **80** 245435
[14] Koppens F H L, Chang D E and Abajo F J G 2011 *Nano Lett.* **11** 3370
[15] Ozbay E 2006 *Science* **311** 189
[16] Boltasseva A and Atwater H A 2011 *Science* **331** 290
[17] Manjavacas A, Marchesin F, Thongrattanasiri S, Koval P, Nordlander P, Sanchez-Portal D and Abajo F J G 2013 *ACS Nano.* **7** 3635
[18] Xia F, Muelle T, Lin Y, Valdes-Garcia A and Avouris P 2009 *Nat. Nanotech.* **4** 839
[19] Sun Z, Hasan T, Torrisi F, Popa D, Privitera G, Wang F, Bonaccorso F, Basko D M and Ferrari A C 2010 *ACS Nano.* **4** 803
[20] Liu M, Yin X, Ulin-Avila E, Geng B, Zentgraf T, Ju L, Wang F and Zhang X 2011 *Nature* **474** 64
[21] Novoselov K S, Geim A K, Morozov S V, Jiang D, Zhang Y, Dubonos S V, Grigorieva I V and Firsov A A 2004 *Science* **306** 666
[22] Miyata Y, Kamon K, Ohashi K, Kitaura R, Yoshimura M and Shinohara H 2010 *Appl. Phys. Lett.* **96** 263105
[23] Liu P, Arai F and Fukuda T 2006 *Appl. Phys. Lett.* **89** 113104
[24] Ribeiro F J, Neaton J B, Louie S G and Cohen M L 2005 *Phys. Rev. B* **72** 75302
[25] Lee G D, Wang C Z, Yoon E, Hwang N M, Kim D Y and Ho K M 2005 *Phys. Rev. Lett.* **95** 205501
[26] Pradhan S C and Phadikar J K 2009 *Phys. Lett. A* **373** 1062
[27] Duplock E J, Scheffler M and Lindan P J D 2004 *Phys. Rev. Lett.* **92** 225502
[28] Lusk M T and Carr L D 2008 *Phys. Rev. Lett.* **100** 175503
[29] Sanyal B, Eriksson O, Jansson U and Grennberg H 2009 *Phys. Rev. B* **79** 113409
[30] Dai X, Li Y, Zhao J and Zhao B 2011 *Physica E* **43** 1461
[31] Yazyev O V and Helm L 2007 *Phys. Rev. B* **75** 125408
[32] Ma Y, Lehtinen P O, Foster A S and Nieminen R M 2004 *New J. Phys.* **6** 68
[33] Gass M H, Bangert U, Bleloch A L, Wang P, Nair R R and Geim A K 2008 *Nat. Nanotechnol.* **3** 676
[34] Banhart F, Kotakoski J and Krasheninnikov A V 2011 *ACS Nano.* **5** 26
[35] Kobayashi Y, Fukui K, Enoki T and Kusakabe K 2006 *Phys. Rev. B* **73** 125415
[36] Ugeda M M, Brihuega I, Guinea F and Gomez-Rodriguez J M 2010 *Phys. Rev. Lett.* **104** 096804
[37] Yan J, Yuan Z and Gao S 2007 *Phys. Rev. Lett.* **98** 216602
[38] Yan J and Gao S 2008 *Phys. Rev. B* **78** 235413
[39] Lian K Y, Sa?ek P, Jin M and Ding D 2009 *J. Chem. Phys.* **130** 174701
[40] Guidez E B and Aikens C M 2014 *Nanoscale* **6** 11512
[41] Cao E, Guo X, Zhang L Q, Shi Y, Lin W H, Liu X C, Fang Y R, Zhou L Y, Sun Y H, Song Y Z, Liang W J and Sun M T 2017 *Adv. Mater. Interfaces* **4** 1700869
[42] Lin W H, Cao E, Zhang L Q, Xu X F, Song Y Z, Liang W J and Sun M T 2018 *Nanoscale* **10** 5482
[43] Nayyar N, Turkowski V and Rahman T S 2012 *Phys. Rev. Lett.* **109** 157404
[44] Mu X and Sun M 2020 *Mater. Today Phys.* **14** 100222
[45] Liu Y, Cheng R, Liao L, Zhou H, Bai J, Liu G, Liu L, Huang Y and Duan X 2011 *Nat. Commun.* **2** 579
[46] Echtermeyer T J, Britnell L, Jasnos P K, Lombardo A and Gorbachev R V 2011 *Nat. Commun.* **2** 458
[47] Takatsuka Y, Takahagi K, Sano E, Ryzhii V and Otsuji T 2012 *J. Appl. Phys.* **112** 033103
[48] Marques M A L, Castro A, Bertsch G F and Rubio A 2003 *Phys. Commun.* **151** 60
[49] Troullier N and Martins J L 1991 *Phys. Rev. B* **43** 1993
[50] Ceperley D M and Alder B J 1980 *Phys. Rev. Lett.* **45** 566
[51] Marinopoulos A G, Reining L, Olevano V, Rubio A, Pichler T, Liu X, Knupfer M and Fink J 2002 *Phys. Rev. Lett.* **89** 076402
[52] Niu J, Shin Y J, Lee Y, Ahn J H and Yang H 2012 *Appl. Phys. Lett.* **100** 061116
[53] Zhang K, Zhang H and Li C K 2015 *Phys. Chem. Chem. Phys.* **17** 12051
[54] Mu X J, Wang J G, Duan G Q, Li Z J, Wen J X and Sun M T 2019 *Spectrochim. Acta A* **212** 188